



Seismic characteristics of hybrid cold-formed steel wall panels

Nima Usefi*, Hamid Ronagh

Centre for Infrastructure Engineering, Western Sydney University, Sydney, Australia

ARTICLE INFO

Keywords:

Cold-formed steel
Square hollow section
Prefab
Truss brace
Response modification factor
Modular
Shear wall

ABSTRACT

The current standards for seismic design of cold-formed steel (CFS) structures are only limited to the lateral force-resisting systems which are not appropriate for mid-rise constructions due to their low shear resistance. Therefore, innovative hybrid CFS systems have recently been proposed and developed in response to the needs of CFS provisions as well as lightweight steel industry in mid-rise construction. This paper presents an experimental program on lateral cyclic behaviour of six full-scale hybrid wall panels with truss structural design and aims to investigate and characterize the seismic performance of this new CFS solution. The performance of the wall panels is compared in terms of seismic characteristics and response modification factor (R factor). A comprehensive comparison between lateral strength to weight ratio of the hybrid panels of this study and 87 previously tested CFS walls is also carried out to investigate the capability of using hybrid walls in modular lightweight steel buildings. The cyclic results demonstrate that the seismic performance of specimens with appropriate truss frame is satisfactory considering their shear strength, ductility and R factor values. The high strength to weight ratio of the hybrid walls of this study compared to the previously tested CFS panels also indicates the hybrid panels are well appropriate for modular lightweight buildings in seismic regions.

1. Introduction

Over the past few years, the development in building automation has led to the invention of many prefabricated cold-formed steel (CFS) wall panels as one of the leading products of modular lightweight steel structures, particularly in mid-rise buildings. A typical CFS wall is generally fabricated from open CFS sections (U and C section profiles). However, it is well acknowledged that the implementation of open CFS sections for lateral bearing systems would result in many types of instabilities during seismic action and consequently reduces the lateral resistance of system [1,2].

The low lateral resistance of traditional CFS wall panels has persuaded many research groups to develop several experimental, numerical and theoretical investigations aiming to improve the lateral performance of CFS walls through bracing and sheathing methods. Strap brace is one conventional method of bracing system for CFS walls where its application has been extensively investigated during recent years [3,4,5]. There are also some new bracing systems such as K bracing [6,7] and truss bracing [8] proposed in the literature which have shown reasonable advantages in terms of ductility and energy absorption during lateral loading. Sheathing, on the other hand, can provide considerable strength and stiffness for CFS shear wall panels. A large number of studies have been carried out to develop new sheathing

materials such as cement board [9], gypsum board [10], wood-based sheathing [11] and steel [12,13] in order to satisfy the requirements of fire resistance and provide lateral and rotational supports to the studs in the plane of the wall. There have also been several attempts to mix other materials such as lightweight mortar and concrete with CFS frames that improve their lateral behaviour and remedy the existing insufficiencies [14–16]. In recent years and in parallel with some attempts for evaluation of the actual behaviour of CFS walls under seismic loading, the effects of bracing and sheathing material on the performance of a CFS system were investigated through shake table tests [17–20]. In addition, significant progress has also been made on the applications of the numerical models for the analysis of the lateral behaviour of CFS wall systems during the past several decades [1,21–26].

Despite the extensive development of research programs on CFS walls in the literature, the current CFS provisions are only limited to shear walls which are only suitable for low-rise buildings. For example, North American standard for seismic design of CFS structural frame (AISI-S400) [27], as the main reference for designing CFS wall panels, only provides guidelines for CFS panels which are restricted by sheathing and framing thicknesses, fastener spacing, screw sizes, and aspect ratio. In addition, the nominal design values tabulated in the current standards are not adequate to be employed for design of a mid-

* Corresponding author.

E-mail address: n.usefi@westernsydney.edu.au (N. Usefi).

Table 1

R factor values according to different CFS codes.

Code	R factor value	Detail
ASCE7 [35]	6.5	Light frame wall sheathed with wood structural panels rated for shear resistance or steel sheets
	4	Light frame wall systems using flat strap bracing
	2	Light frame wall with shear panels of all other materials
FEMA P-1050 [32]	6.5	Light frame wall with shear panel
	4	Light frame wall with diagonal braces (special requirements)
	3	Light frame wall with diagonal braces or other systems such as K brace
UBC [33]	2.8	Light frame wall systems using flat strap bracing
	5.5	Walls sheathed with wood-based panels
	4.5	Other types of lightweight walls
AS/NZS 4600 [38]	2	When CFS members are used as the primary seismic lateral load-bearing system,
	$2 < R < 3$	Walls with no special requirements
	$3 < R < 7$	Walls with implementation of detailing
NBCC [36]	2.55	Gypsum wall with wood base panel
	2.6	Walls with strap brace and limited ductility
	1.6	Conventional structures with strap
IBC [34]	6.5	Shear walls sheathed with wood panels or steel sheets
	2	Walls with other types of sheathings
	4	Walls with strap brace

rise CFS building. Therefore, to improve the relevant design codes towards mid-rise construction, development of stronger CFS shear walls with higher shear resistance and ductility is deemed necessary.

New hybrid CFS wall composed of open CFS sections and square hollow section (SHS) is one of the recent inventions proposed to enhance the shear wall resistance by replacing C-shaped CFS section with square steel tube [28–30]. This system supplies higher buckling capacity compared to traditional CFS walls (due to closed section components) and also offers a relatively high strength to weight ratio compared to the previously proposed systems. In addition, bearing and pull-out resistance of screws are increased when SHS is employed in the wall assembly. To date, Western Sydney University's research program on CFS hybrid wall has engaged in developing a database of experimental data for various hybrid panel configurations in an attempt to evaluate the performance of these shear walls under both monotonic and cyclic loads [28–30]. In the first phase of this research, the monotonic behaviour of the CFS hybrid panels was investigated through eleven full-scale specimens [30]. However, it is also essential to carry out cyclic tests to derive seismic characteristics such as response modification factor (R factor) by establishing correct relationships. Therefore, an experimental program was developed to test six hybrid CFS wall specimens under reversed cyclic loading to promote the use of CFS lateral systems in mid-rise buildings. The tasks conducted in this research included the following steps:

- i) Testing full-scale single-storey hybrid CFS specimens, which can provide higher shear capacity and ductility than CFS walls listed in the CFS regulations,
- ii) Achieving preliminary design parameters and nominal shear resistance values,
- iii) Comparing hybrid CFS walls in this study against 87 previously tested CFS wall panels from 28 references in terms of strength to weight ratio,
- iv) Determining seismic force modification factors, R_d and R_o according to the Federal Emergency Management Agency (FEMA) FEMA356 [31] and FEMA P-1050 [32] methodologies.

2. R factor in CFS regulations

R factor is an important parameter that is required to investigate the induced seismic force and to determine the reduced lateral loads for design of a building. The values of R factor for CFS buildings are proposed by several codes including Uniform Building Code (UBC) [33], International Building Code (IBC) [34], FEMA P-1050 [32], American Society of Civil Engineers (ASCE) ASCE07 [35] and National Building

Code of Canada (NBCC) [36]. However, these codes do not necessarily provide equal R factor values for similar CFS buildings. The disagreement between R factor values of the mentioned regulations is mainly due to the different approach of calculating R factor as well as the different employed bilinear curve. In some provisions such as the European code for seismic design [37], the design of CFS walls is based on hot-rolled steel formulations and also the design of sheathed CFS walls is not possible if the sheathing material is different from steel.

Table 1 shows the values of the R factor identified by different CFS codes. As shown in this table, there is not a general agreement on the R factor value for CFS solutions, and especially, there is no R factor value in these regulations for systems braced with CFS truss elements. Therefore, this study also aims to estimate the R factor for an SHS truss-braced CFS hybrid wall through FEMA 356 [31] and FEMA P-1050 [32] procedures and based on the experimental results.

3. Experimental program

3.1. Test specimens

Six full-scale CFS wall panels with square geometry of 2400 mm were assembled for the experimental test, as shown in Fig. 1. The CFS tracks were selected of U channels with 92 mm web, 50 mm flange and 1.15 mm thickness. The lipped C channels with 92 mm web, 36 mm flange, 10 mm lip and 0.55 mm thickness were also used as the CFS studs and noggins. The truss skeleton was made of SHS with a dimension of 89 mm × 89 mm × 2 mm. Table 2 summarizes the configuration details of the hybrid wall panels. The steel frame components were assembled with 5.5 mm thread diameter self-drilling screws. Three specimens were sheathed with 10 mm thick gypsum wall board (GWB) to determine the influence of sheathing board on the seismic performance of the hybrid shear wall. The GWB was installed on the steel frame through 12-gauge self-drilling screws with 35 mm long spaced at 300 mm centre to centre at the perimeter and field studs. The material properties of the wall components summarized in Table 3 were also obtained by tensile coupon tests. Three coupons were tested for each wall component and the mean values were then recorded. The screws shear and tensile strengths were 9.1 KN and 15.8 KN, respectively, which were obtained from screw technical guide [39].

As illustrated in Fig. 1, specimens HW-C1 and HW-C2 (H for Hybrid, W for Wall, C for Cyclic test) were fabricated from one SHS truss frame and three open-section CFS studs. The unique difference between these two specimens is that the truss in the specimen HW-C2 is 180° turned over compared to HW-C1. Specimen HW-C3 is also similar to the specimen HW-C2, but in order to mitigate the overturning of the wall panel

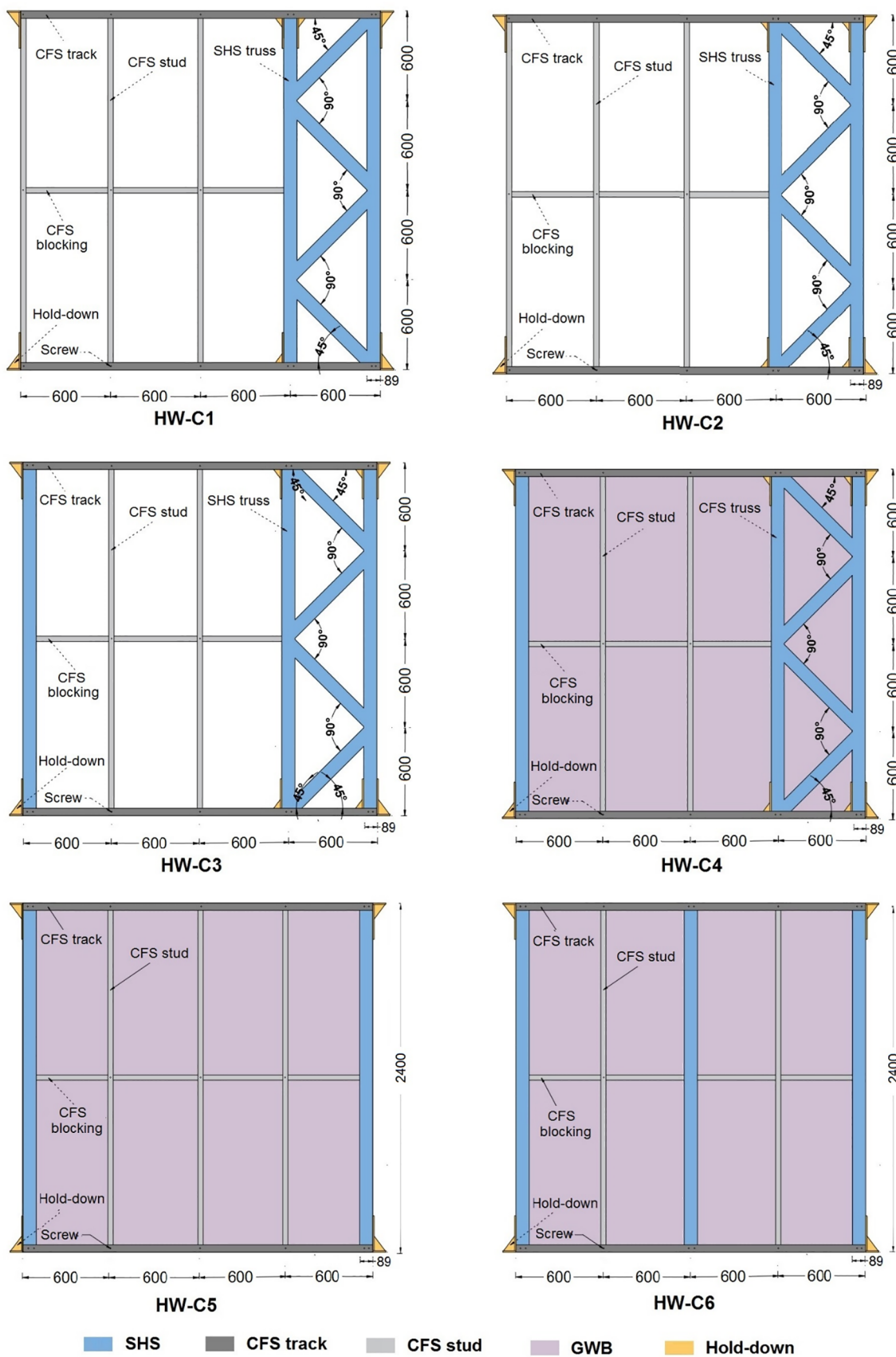


Fig. 1. Schematic of hybrid walls (all dimensions in mm).

Table 2
Test specimens.

Specimen	GWB	SHS (mm)	CFS (mm)	
			Stud	Track
HW-C1		89 × 89 × 2	92 × 36 × 0.55	92 × 50 × 1.15
HW-C2				
HW-C3				
HW-C4	✓			
HW-C5	✓			
HW-C6	✓			

as well as to provide better seismic performance, SHS element was employed for the chord stud of the specimen HW-C3. GWB was also attached to the HW-C3 and tested as a new wall, HW-C4, to investigate the influence of finishing material on the cyclic behaviour of the hybrid wall. Specimens HW-C5 and HW-C6 were fabricated to provide insight into the impact of using single SHS as the chord and field studs, and their results were only employed to demonstrate that the truss structure is the leading solution of the proposed hybrid panels. Hold-down device type B used for monotonic study [30] of these wall panels was also employed for cyclic tests where two 18 mm high strength bolts were utilized to connect the SHS members to the hold-down. The comprehensive details of the wall to floor connections (hold-down type B) as well as the discussion on the friction and bearing between the hold-down and the SHS element can be found in Section 3.3 of the monotonic study on these wall panels [30].

3.2. Test setup and loading protocol

The testing rig for performing the cyclic tests is displayed in Fig. 2. The tracks of the wall specimens were attached to the loading and reaction beams of the testing rig using 18 mm diameter high-strength bolts. The rigid foundation was simulated by fixing the bottom reaction beam on the floor. Four lateral supports were utilized at both sides of the loading beam (two at each side) to control the out of plane movement of wall panels. The lateral cyclic load was applied to the loading beam through a hydraulic jack with ± 120 S and 500 KN capacity. This hydraulic jack was then equipped with a load cell of 200 kN capacity. A hinged connection was employed for connecting the loading beam to the hydraulic jack to prevent any undesirable damage on the load cell. Eight linear potentiometers (LP) were also placed at different locations to record the vertical and horizontal deformations of the wall panels, as illustrated in Fig. 2. The lateral displacement of the actuator was recorded through a linear variable displacement transducer (LVDT).

The method B (International Standards Organization protocol, ISO) and method C (CUREE protocol) of ASTM E2126 [40] standard have been extensively used for testing of lightweight CFS wall panels. Since method B of ASTM E2126 standard [40] is more frequently used for CFS walls with 2400 mm to 2400 mm dimension (same as hybrid walls in this study), this method was implemented for cyclic loading of the wall panels of this study. ASTM E2126 [40] specifies two loading patterns for this loading protocol: a) single cycles at 1.25%, 2.5%, 5%, 7.5% and 10% of the ultimate displacement (Δ_m); and b) three cycles at displacements of 20%, 40%, 60%, 80%, 100% and 120% of the ultimate displacement (Δ_m). Δ_m is defined as the ultimate displacement capacity specified from the monotonic tests. However, it was not possible to

capture the Δ_m value based on the monotonic test results as the applied lateral load did not decline to 80% of the peak load because of the stroke limit of the hydraulic jack [30]. The 2.5% maximum allowable storey-drift limit (60 mm for a 2400 mm wall) was therefore considered as the value of Δ_m for cyclic tests. Table 4 and Fig. 3 show the regime of cyclic loading in this study. The loading rate was 2 mm/s, which is within the displacement range of 1–63 mm/s recommended by ASTM E2126 [40].

4. Experimental results

4.1. Observations and failure modes

According to the observations obtained during the tests, elastic deformation in SHS elements occurred for all specimens throughout the initial stages of loading. By increasing the displacement amplitudes, plastic deformations were formed at the hold-down locations of the specimens with SHS truss element, HW1, HW2, HW3 and HW4.

In general, all unsheathed walls demonstrated similar failure mechanism. During the final stages of loading on HW-C1 and HW-C2, the SHS truss element on the tension side was lifted up from the reaction beam which was followed by the upward deformation of the bottom track and consequently local failure of the track at the location of the track to SHS connection. The reason for this type of failure can be justified by the lack of applying vertical load, which allows overturning of the wall and therefore causes undesirable deformations. Overturning of the wall panel in specimens HW-C1 and HW-C2 also resulted in hole elongation of SHS at hold-down connection which was due to the bearing between the edge of the SHS hole, the bolt and the hold-down. Fig. 4 shows the uplift movement on the tension side of the SHS truss and the plastic deformations at the location of hold-downs. As shown in this figure, the general failure mechanism of specimens HW-C1 and HW-C2 is nearly similar. In specimen HW-C3, utilizing one single SHS chord at the other side of the wall panel could reasonably control the unfavourable overturning of the panel. Accordingly, the intensity of failure at the connection location was significantly mitigated. New investigation methods [41,42] can be utilized for the optimum design of connections in the hybrid systems to eliminate the unfavourable connection failure. The typical track failures in the unsheathed wall panels were also observed during the cyclic tests, as shown in Fig. 5.

The observations in test specimen HW-C4 with GWB showed that utilizing sheathing board on the wall face can lead to superior force transmission between wall components, including SHS elements and CFS members compared to when sheathing is not employed (specimen HW-C3). In this specimen, the localized failures observed in HW-C1, HW-C2 and HW-C3 were prevented or delayed due to the distribution of forces between the steel elements by GWB. Besides, the uplift force in the tension side of SHS truss was restricted because of GWB, which prevented the undesirable failures such as the bottom track upward deformation and elongation of the hole at the hold-down connections. When lateral displacement was applied to the specimen HW-C4, bearing and pull through damage in the GWB as well as screw tilting in the frame occurred primarily due to the non-uniform deformation between the GWB and the framing elements. Tilting of screws occurred first when loading was applied initially, and then the failure mechanism was followed by other types of failure modes such as bearing and pull through of screws. The screw failures around the perimeter elements

Table 3
Material properties.

Section	Nominal thickness (mm)	Yield stress, f_y (MPa)	Ultimate stress, f_u (MPa)	F_u/F_y	Elongation (%)
SHS	2	352	438	1.24	15
CFS Stud and blocking	0.55	305	338	1.11	18
CFS track	1.15	295	332	1.12	18

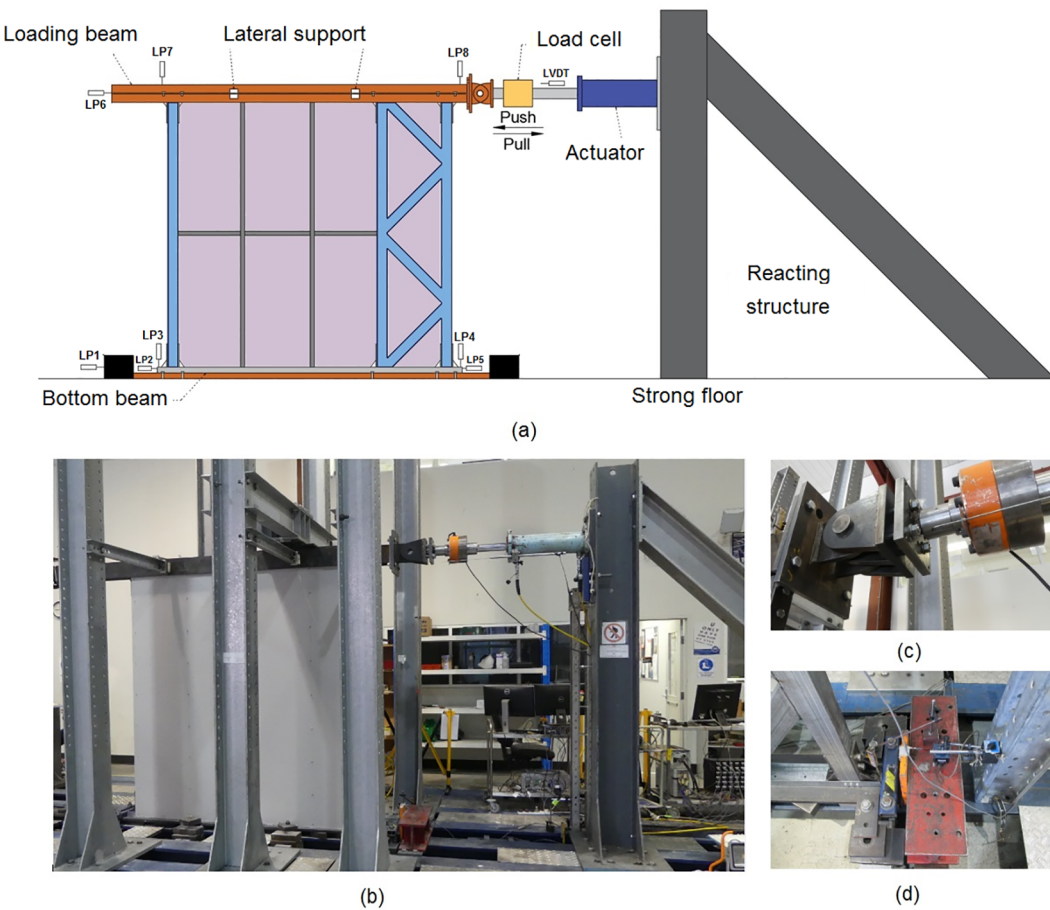


Fig. 2. Test rig: a) schematic of the test rig, b) actual test rig, c) loadcell and hinge connection d) restrain and LPs.

Table 4
Cyclic loading regime, Method B - ASTM E2126.

Pattern	Step	Minimum Number of Cycles	Amplitude, % Δ_m (%) 60 mm)	Actuator stroke (mm)
1	1	1	1.25	0.75
	2	1	2.5	1.5
	3	1	5	3
	4	1	7.5	4.5
	5	1	10	6
2	6	3	20	12
	7	3	40	24
	8	3	60	36
	9	3	80	48
	10	3	100	60
	11	3	120	72
	12	3	140	84

were found to be more severe than the failures of screws near the interior studs. This is because the perimeter screws were under higher differential displacement compared to field screws. At higher load increments, the sheathing was gradually subjected to intensive damage around the location of screw connections which was followed by partial separation of the GWB from the framing elements (pull-through failure). This detachment resulted in the lack of rigid body movement of the wall panel and therefore decreased the lateral stiffness of the wall panel. Fig. 6 shows different failures of the specimen HW-C4. For the specimen HW-C6, when the field stud was replaced by a single SHS, gypsum splitting at field stud was much less than specimen HW-C5 due to the implementation of thicker elements which can control the tilting of screws.

4.1.1. Hysteresis response and envelope curves

Figs. 7 and 8 display hysteresis and envelope curves of wall panels under cyclic loading, respectively. The net displacement was determined according to a method presented in [30], which considers wall sliding as well as deformations due to rigid body rotation of the panel. It is also notable that because of the limitation of actuator stroke, the failure of wall panels could not be reached during the test, and therefore, the maximum shear resistance was recorded at a drift of 3.5%.

The hysteresis results of HW-C2, HW-C3 and HW-C4 indicate that the walls under pulling phase provide less shear resistance compared to walls under pushing phase. This difference is generally as a result of two particular factors: One main reason is that the walls were first under pushing deformation and consequently, experienced inelastic deformations which directly affected the walls' ability to bear the lateral load in the reverse pulling direction. The second reason is attributed to the unsymmetrical structure of hybrid panels and particularly the SHS truss part. The SHS truss on tension side was restrained by two connectors when wall panel was under pushing phase, while only one hold-down was employed on the tension side of the truss when pulling load was imposed to the panel. The difference between pushing and pulling phases of specimens HW-C5 and HW-C6 is relatively negligible owing to their symmetrical configuration.

Comparing the energy dissipation of the first and third cycle of the specimens HW-C4 and HW-C5 indicates that the energy dissipation in consecutive cycles of identical displacement for a hybrid wall with truss brace is more than a hybrid panel in the absence of truss frame. It is also prominent to note the energy dissipation trend in cycles with the same displacement amplitude for bare hybrid wall panel is different from wall panels with GWB sheathing. The variation in energy dissipation in

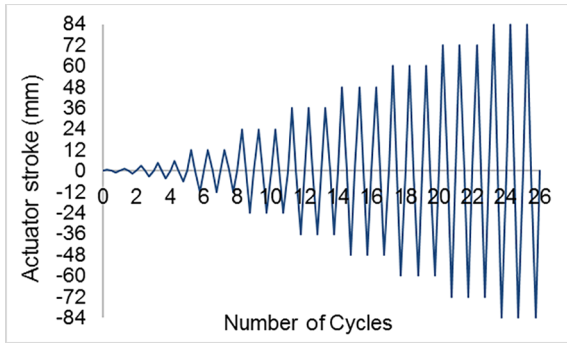


Fig. 3. Cyclic load protocol.

identical displacement for wall panels with GWB sheathing is more evident than panels without GWB. This is mainly because GWB loses much of its performance in the first cycle and therefore, the energy absorption is significantly reduced in second and third cycles of the same amplitude. Accordingly, in large lateral displacements, the strength and stiffness degradation between the first and second cycle is considerably higher than the second and the third cycles of the same displacement amplitude. Notably, the energy dissipation and ductility of the proposed hybrid system can also be increased by modifying the diagonal SHS elements to a fuse element according to the capacity-based design approach [43].

4.1.2. Analysis of the test results

The Equivalent Energy Elastic-Plastic (EEEP) model is employed for establishing design parameters of hybrid panels under cyclic load. The results include the test peak point, elastic point, yield point and ultimate point. The peak point (Δ_{\max} , P_{\max}) is defined as the maximum load and the corresponding displacement on the envelope curves. The elastic point (Δ_e , P_e) is positioned at 0.4P_{max}, and the yield point (Δ_y , P_y) is achieved through EEEP method according to the method given in AISI-S400 [27]. The ultimate point (Δ_u , P_u) is determined as the location of the 80% post-peak load; however, the ultimate point could not be achieved since the wall panel strength did not drop within demand displacement range and therefore, the pick point is considered as the ultimate point of all hybrid panels.

Initial stiffness, ductility factor and absorbed energy are determined from the test results for each reversed cyclic test in pushing and pulling phases, and an average value is then obtained. Ductility factor is specified by the ratio of the ultimate to the yield displacement. Energy absorption is characterized as the area under the backbone curve, and

the lateral stiffness is defined as the secant stiffness to a load of 0.4P_{max}, as per AISI recommendation [27]. The design values captured from each wall panel under cyclic loading are presented in Table 5.

Fig. 9 shows the comparison of energy absorption, stiffness and maximum shear capacity under pushing and pulling phases for hybrid wall panels in this study. As shown in this figure, the SHS truss skeleton in both HW-C1 and HW-C2 is able to provide sufficient resistance. In general, the overall average values of HW-C2 are higher than HW-C1, which indicates the truss direction in the panel can slightly affect the performance of the hybrid wall. In specimen HW-C3, by using the single SHS element at the other end of the wall, the wall panel provides superior performance in terms of the maximum lateral resistance and the energy absorption compared to HW-C2. The average increase in maximum strength, due to the replacing the CFS stud with SHS, in both positive and negative phases is about 20% and 31%, respectively. Using GWB in HW-C4 also leads to a significant increase in the peak load, initial stiffness, energy absorption and ductility than the wall without sheathing (HW-C3), which is attributed to the restrictive effect of GWB on the wall panel and screw connections. Specimens HW-C5 and HW-C6 were only tested to compare the impact of using a single SHS element as a field stud. The ductility ratio, stiffness and energy absorption of the specimen HW-C6 show that replacing CFS field stud with SHS stud leads to increase in the shear capacity of the sheathed shear wall.

The overall comparison of all wall panels shows that specimens HW-C5 and HW-C6 are not suitable for mid-rise structures as their strengths are relatively low compared to their weights. This indicates that the performance of the hybrid wall is mainly determined through the truss structure of SHS elements. It is notable that the obtained results of the hybrid wall panels in the lack of vertical load are conservative compared to when gravity load is applied on the wall panels. Applying gravity load on panels would increase the stiffness and shear strength of the system mainly due to two main reasons: a) the membrane action of the sheathing generated under vertical load would provide superior performance for the entire system, and b) applying vertical load would control the uplift and overturning of the walls which results in less undesirable failure modes such as hole elongation in hold-down [44]. It should also be noted that the rotation and overturning of the wall panels in an actual building do not occur due to the assumption of rigid floor diaphragm.

4.2. Comparison between cyclic and monotonic results

Comparison of the cyclic test results of this study against the monotonic results obtained from the previous study [30] is shown in Fig. 10. The results are compared in terms of maximum strength at

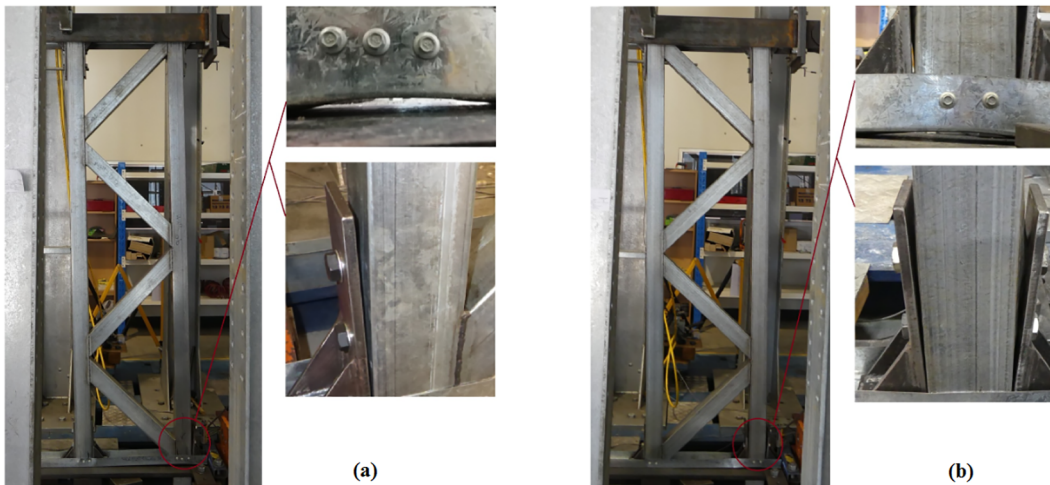


Fig. 4. Deformation and failure in: a) HW-C1 b) HW-C2.

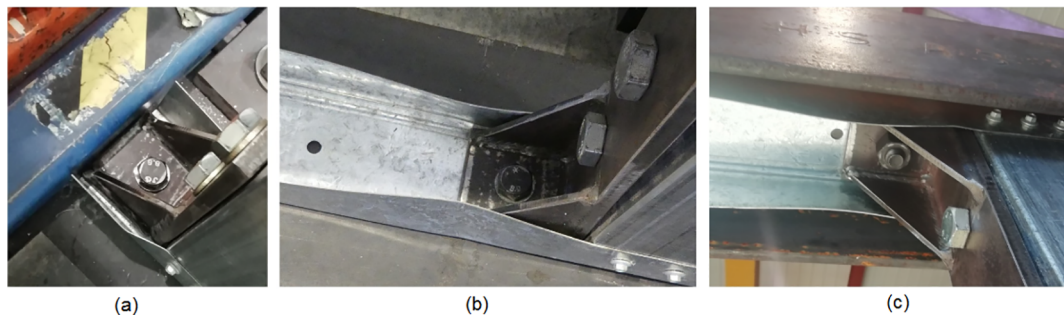


Fig. 5. Track deformation at hold-down location: a) bottom- end hold-down, b) bottom-middle hold-down b) top-middle hold-down.

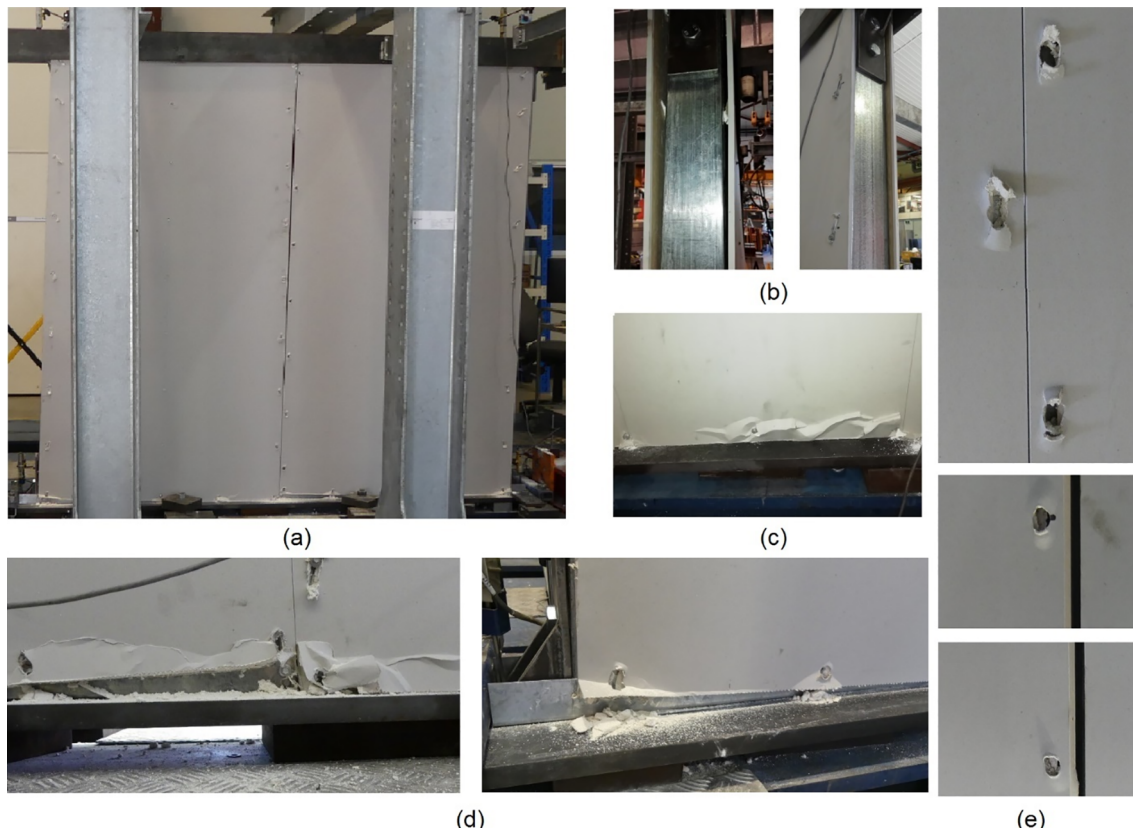


Fig. 6. Failure modes of the specimen HW-C4: a) Overall deformation of GWB board, b) detachment of the GWB from the frame, c) bearing failure of GWB, d) Tear-out sheathing failure and GWB crashing, e) Pull-through of the screw.

2.5% and 3.5% inter-storey drifts as well as stiffness and ductility. The comparison is only provided for pushing phase of the specimens HW-C2, HW-C3, HW-C4 and HW-C5 since no monotonic test was conducted for the specimens HW-1 and HW-6.

The overall response and trend of the hybrid walls under cyclic loading is similar to that obtained from monotonic loading, both with ascending behaviour. The comparison of maximum strength at different inter-storey drifts indicates that the unsheathed wall panels have captured about similar shear strength values for cyclic and monotonic tests. However, for sheathed panels (HW-C4 and HW-C5), the shear strength achieved by the cyclic load is between 4% and 12% lower than the monotonic results. This is mainly due to the strength degradation of GWB and its corresponding failures during the cyclic loading protocol. In terms of stiffness and ductility, the unsheathed walls can provide almost equal performance in cyclic and monotonic tests, while a considerable difference between monotonic and cyclic results (stiffness and ductility) is obtained for sheathed wall panels.

4.3. Comparison with the test results from other researchers

Based only on the load-displacement characteristics of the CFS walls, it is challenging to identify whether a wall panel is sufficiently qualified for a lightweight or modular building in high seismic regions [45]. Strength to weight ratio (S/W) is recognized to be as a critical parameter for evaluating the system in terms of strength and weight relationship and comparing the effectiveness of the structural components for modular or prefabricated lightweight steel buildings.

In order to investigate the S/W ratio of hybrid walls in this paper, 87 tested CFS wall panels from 28 previous studies along with the hybrid walls presented in this paper are compared. The parameters used for this comparison include the total frame weight, the maximum strength before or at 2.5% maximum allowable lateral drift, the displacement at maximum strength, elastic stiffness and S/W ratio. The limitation of 2.5% maximum allowable drift is accounted for this comparison since the maximum shear resistance of some wall panels was reached after this maximum allowable drift.

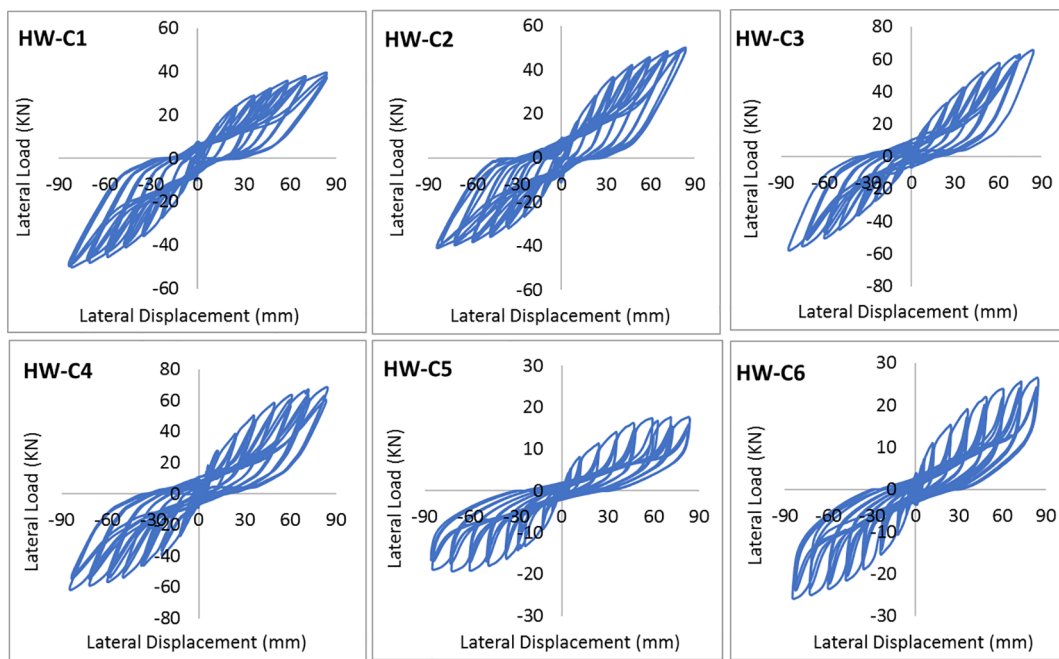


Fig. 7. Load–lateral displacement hysteresis curves of the specimens.

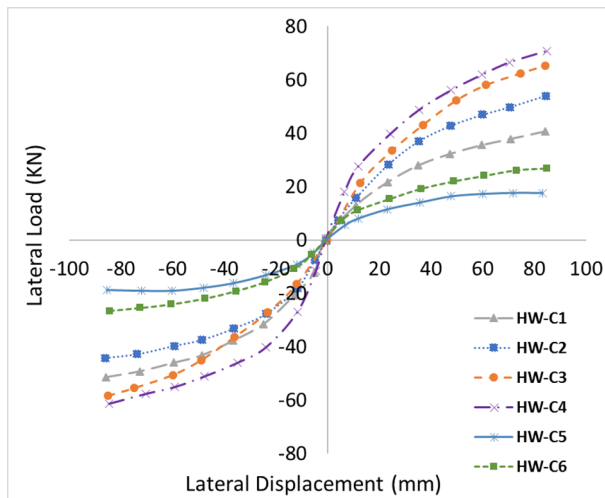


Fig. 8. Envelope curves.

In order to undertake a reasonable comparison between the lateral behaviour of hybrid shear wall panels in this paper and the other CFS walls in the previous studies, the following assumptions are taken into account:

- The screws weight is ignored in measuring the total weight of the walls.
- The maximum strength is considered as the pick point of the load–displacement curve before or at 2.5% maximum allowable lateral drift. For walls with both monotonic and cyclic results, the maximum strength value of either cyclic or monotonic response is considered. The average amount of pushing and pulling phases is employed for this comparison.
- Only wall panels with 2400 mm width or longer are considered for this evaluation. This is in compliance of wider wall panel can provide higher shear resistance which can be a conservative comparison for hybrid walls with 2400 mm length.
- Wall panels with different sheathing materials are employed for this

comparison. Although Plywood, Oriented Strand Board (OSB) and steel sheets are of greater shear stiffness than the GWB, the hybrid wall with GWP in this study (HW-C4) places in the conservative side of this comparison.

- The density of wall components (framing, sheathing and infilled materials) are extracted from either the original reference or reliable industry references.

4.3.1. Comparison of unsheathed walls (HW-C2, HW-C3)

Table 6 shows the characteristics of CFS walls which are relying only on bracing systems. Truss brace, strap brace, knee brace, k brace and hybrid systems tested by other researchers along with specimens HW-C2 and HW-C3 of this study are taken into consideration for this comparison. Fig. 11 also shows the S/W ratio for the wall panels without sheathing board.

As shown in this figure, the S/W ratios of HW-C2 and HW-C3 are basically higher than other CFS braced wall panels tested in other studies (except WHE by Fiorino et al., [3]). This indicates that besides the superior loadbearing capacity of the hybrid walls in this study, they can also offer the benefits of a lightweight system by keeping the weight and size of the walls reasonably low which fully satisfies the requirement of prefabricated and modular structures.

Only specimen WHE tested by Fiorino et al. [3] has provided higher S/W ratio than hybrid panels in this study; nevertheless, the total weight of this former wall is nearly four times greater than HW-C2 in this study (217 Kg for the WHE [3] and 54 Kg for the HW-C2 in this study). Although innovative wall panels such as specimen WHE [3] can offer remarkable seismic performance, the high mass of the entire wall intensifies the dead load of the wall panel and as a result the seismic base shear of the building during an earthquake. Besides, the higher weight of the wall panel would cause some difficulties during lifting and installation of panels and limits the prefabrication advantages.

It is also interesting to note that, unlike hybrid walls in this study, the maximum shear resistance of the majority of CFS walls has reached before the 2.5% maximum allowable drift demonstrating that the hybrid wall is characterized with high ability to absorb energy well beyond its design requirements. Considering that enhancing shear wall length can accordingly increase the stiffness and lateral strength, specimens III [46], V [28] and HWPS [29] even with higher length than

Table 5
Design values for hybrid walls.

Specimen		Δ_e	P_e	Δ_y	P_y	$\Delta_{max} = \Delta_u$	$P_{max} = P_u$	K	μ	E
HW-C1	(+)	15.0	16.3	30.9	33.5	84	40.7	1.09	2.7	2298
	(-)	12.9	20.5	28.1	44.7	84	51.3	1.59	3.0	3128
	Ave.	14.0	18.4	29.5	39.1	84	46.0	1.34	2.8	2713
HW-C2	(+)	16.0	21.6	33.3	45.1	84	54.1	1.35	2.5	3036
	(-)	11.3	17.7	24.4	38.1	84	44.2	1.56	3.4	2738
	Ave.	13.7	19.7	28.8	41.6	84	49.2	1.46	2.9	2887
HW-C3	(+)	16.5	26.1	34.0	53.8	84	65.2	1.58	2.5	3604
	(-)	18.0	23.2	37.7	48.7	84	58.1	1.29	2.2	3172
	Ave.	17.3	24.7	35.9	51.3	84	61.7	1.44	2.3	3388
HW-C4	(+)	12.0	28.3	24.3	57.5	84	70.8	2.36	3.5	4127
	(-)	10.0	24.5	20.8	51.0	84	61.3	2.45	4.0	3753
	Ave.	11.0	26.4	22.6	54.2	84	66.1	2.41	3.7	3940
HW-C5	(+)	9.5	7.1	26.0	19.3	71	17.6	0.74	2.7	1120
	(-)	9.3	7.6	27.2	22.2	71	19.0	0.82	2.6	1275
	Ave.	9.4	7.3	26.6	20.8	71	18.3	0.78	2.7	1198
HW-C6	(+)	11.0	10.7	22.7	22.1	84	26.7	0.97	3.7	1604
	(-)	12.9	10.6	27.2	22.3	84	26.5	0.82	3.1	1573
	Ave.	12.0	10.6	25.0	22.2	84	26.6	0.90	3.4	1589

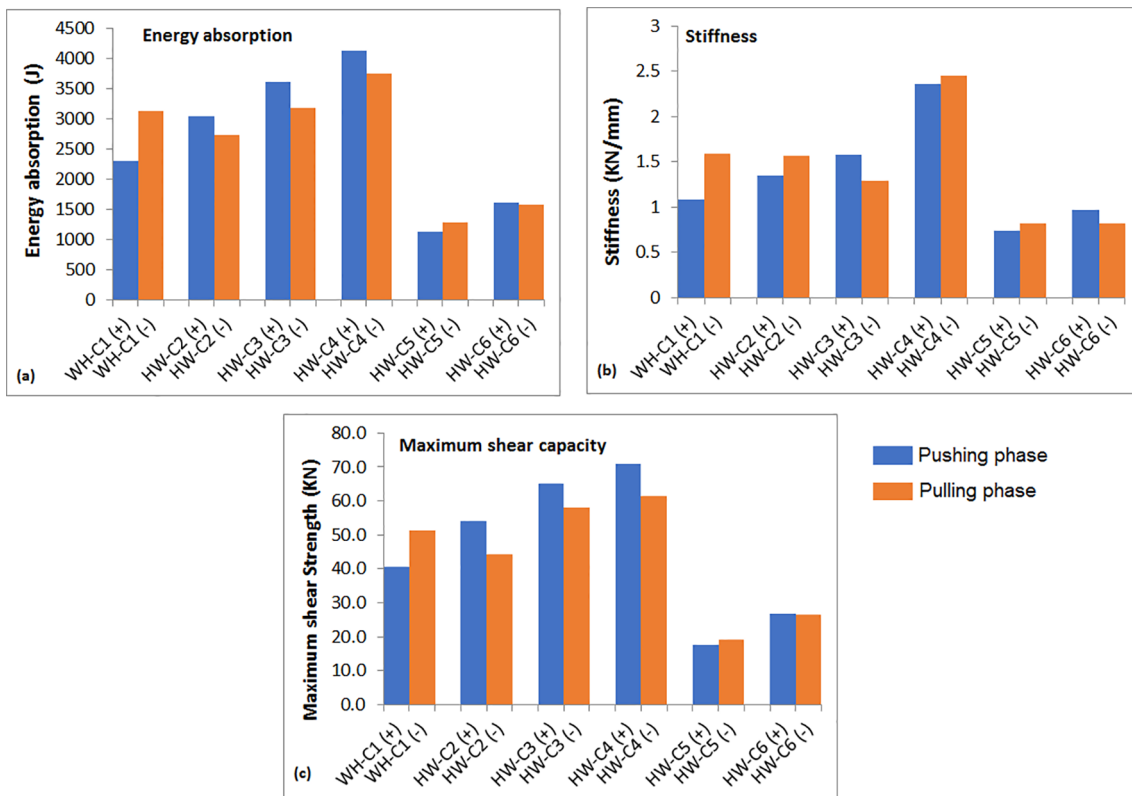


Fig. 9. Comparison of different parameters in pushing and pulling phases: a) Energy absorption b) Stiffness c) Maximum shear capacity.

hybrid walls cannot provide better performance compared to the hybrid panels in this paper.

4.3.2. Comparison of sheathed walls (HW-C4)

The comparison of the wall panels with various sheathing materials along with specimen HW-C4 with GWB in this study is also provided in Table 7. In some specimens, infill material such as concrete or cement grout has been used to increase the shear resistance of the panel. Fig. 12 illustrates the S/W ratio for the sheathed wall panels.

Comparison of the maximum displacement values in Table 7 indicates that the sheathed hybrid panel (HW-C4) is also described with high ability of energy absorption to be used for mid-rise buildings in high seismic regions. This again proves that the SHS elements in the form of truss structure can enhance the seismic performance as well as

energy absorption through employing diagonal members. Except for wall panels WA1 [14], FFM-O09-FO [49], FFM-O12-FO [49], H3 [50] and D-C-3 [11]; the S/W ratio of the sheathed HW-C4 in this study is basically up to 860% higher than that of the wall panels in Table 7. The lower S/W ratio of the HW-C4 compared to specimens WA1 [14], FFM-O09-FO [49], FFM-O12-FO [49], H3 [50] and D-C-3 [11] can be attributed to this point that GWB has been utilized for face sheathing of this wall which provides lower stiffness and lower resistance compared to ply bamboo, fibre cement and OSB sheathing materials. The separate comparison on wall panels only with GWB sheathing provided in Fig. 12 demonstrates that the S/W ratio of the HW-C4 is more than 2 to 10 times greater than that of gypsum sheathed walls in the literature. Besides, specimens WA1 [14] has been filled with concrete material, which can significantly improve the strength and rigidity of the wall

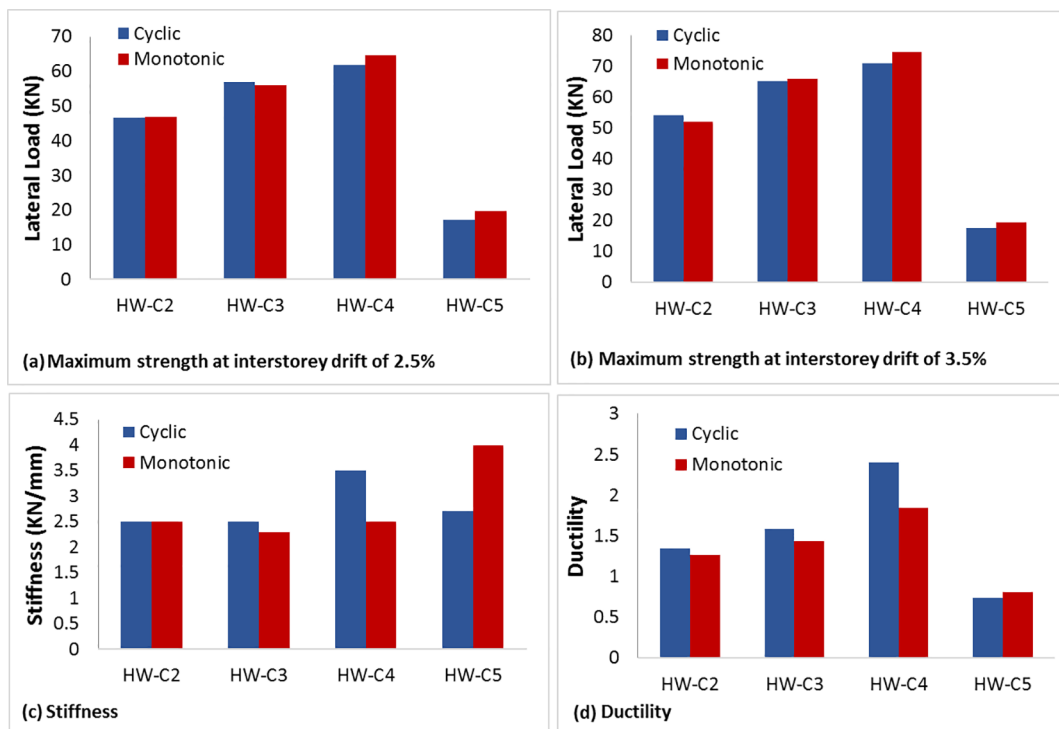


Fig. 10. Comparison between cyclic and monotonic results: a) maximum strength at 2.5% drift, b) maximum strength at 3.5% drift, c) stiffness, d) ductility.

panel. The hybrid wall, on the other hands, is less dependent on the sheathing or infilling material resistance and is more relied on the steel frame components.

The results of Fig. 12 and Table 7 also reveal that in terms of structural performance the proposed hybrid CFS system in this study gives the same design and construction flexibility as many new CFS wall panels, while it offers the advantage of lightweight prefabrication, manufacturing, transportation and installation. In addition, the hybrid CFS method is relatively more cost-effective, which is mainly due to less material used. The shorter time of providing a dry all-steel wall such as the hybrid wall in this study compared to wall panels filled with concrete, foam and mortar can also have a positive effect on reduction of cost and earlier return on investment.

5. Evaluation of R factor

In this paper, the proposed method by FEMA 365 [31] and FEMA P-1050 [32] is employed to estimate the R factor for hybrid CFS walls. The hybrid wall envelope curve results are utilized to determine the lateral characteristics of the hybrid system through preliminary analysis of the R factor. As stated in FEMA P-1050 [32], the R factor can be obtained by two main parameters: ductility reduction factor (R_d) and structural over-strength factor (Ω_0). R_d demonstrates the ability of structure to dissipate energy through inelastic response. Ω_0 considers the possible sources that may provide additional strength beyond its nominal value. Then, the R factor can be defined as:

$$R = R_d \times \Omega_0 \quad (1)$$

$$R_d = \frac{V_e}{V_y}, \quad \Omega_0 = \frac{V_y}{V_s} \quad (2)$$

where V_e is the maximum base shear that creates in the system if it is to remain in the elastic range and is calculated based on the equal energy concept as prescribed by FEMA [32], V_y is determined as the idealised yield strength and V_s corresponds to the first significant yield strength, which is defined as a node on the envelope curve where the structural response begins to considerably diverge from the elastic reaction. As shown in Fig. 13, the key components of the R factor are identified through the concept of equal energy which indicates the energy under elastic response of a system is equal to the energy of the idealised bilinear force-displacement curve.

Table 8 shows the test-based values of R factor components captured by the experimental results. The table shows that the R factors for hybrid walls without sheathing (HW-C1, HW-C2 and HW-C3) range between 5.4 and 7.1; with average of 6.1. For the hybrid walls with SHS truss frame (HW-C1 to HW-C4), the R factor is mainly affected by the overstrength factor ranging from 3.5 to 4.7. The ductility factor of the braced hybrid walls is also between 1.5 and 1.9. For the unbraced walls, on the other hands, the R factor mostly relies on the value of the ductility factor. Analyzing the R factor values also indicates that there is a considerable difference between the R factor of specimens with and without GWB. Taking into account that the shear strength of the wall panel with GWB material (HW-C4) is about 1.16 times than the capacity of the bare panel (HW-C3), the R factor value is 1.3 times higher when GWB is utilized on a braced hybrid wall. This again demonstrates the constructive impact of utilizing GWB for the hybrid panels.

Comparing the R factors of this study with the prescribed values of the R factor in CFS regulations presented in Table 1 shows that the hybrid wall panels meet the current provisions in terms of response modification factor.

It is notable that the test-based R factor is affected by different structural parameters and is not merely relied on the maximum strength

Table 6

Previously tested braced walls by different researchers.

Author, Reference	Bracing system	Specimen ID	Span (m × m)	Frame weight (Kg)	Maximum strength (kN)	Maximum Displacement (mm)	Elastic stiffness (kN/m)
Tian et al., [13]	Truss brace	Configuration 4	2.4 × 3.0	139	47	31	1.29
Accorti et al., [9]		G6-XX2	2.4 × 3.0	79.2	13	75	0.50
Iuorio et al., [4]	Strap brace	G9-XX2	2.4 × 3.0	89.8	36	75	2.61
		WHD	2.4 × 2.7	208.2	121	67.5	5.53
		WLD	2.4 × 2.7	114.3	62	67.5	4.10
		WLE1	2.4 × 2.7	112.7	70	33	4.00
Fiorino et al., [3]		WHE	2.4 × 2.7	217.1	198	61.3	5.60
		WLE2	2.4 × 2.7	137.5	102	65.5	3.40
Al-Kharat and rogers, [47]		2C	2.44 × 2.44	56.4	35	60	1.40
		4C	2.44 × 2.44	95.3	60	44	2.10
		6C	2.44 × 2.44	125.7	85	40	3.60
Serrette et al., [10]		Type A	2.44 × 2.44	40.2	13	60	1.20
Dubina, [46]		III	3.6 × 2.44	107.0	53	18	2.70
Moghimi and Ronagh, [5]		DA2	2.4 × 2.4	16.0	4	60	0.10
		DA1	2.4 × 2.4	16.0	4	60	0.10
		DA4	2.4 × 2.4	21.0	9	60	0.18
		DB4	2.4 × 2.4	20.5	4	60	0.09
		DB1	2.4 × 2.4	15.7	5	60	0.08
Liu et al., [16]		F-XB	2.4 × 3.0	54.8	27	29	1.50
Zeynalian and Ronagh, [48]	Knee brace	F-KB	2.4 × 3.0	45.1	3	57	0.10
		N1	2.4 × 2.4	24.0	2	60	0.06
		N2	2.4 × 2.4	23.4	2	30	0.10
		N3	2.4 × 2.4	23.6	2	46	0.90
		N4	2.4 × 2.4	23.2	2	34	0.90
Pourabdollah et al. [6]	K brace	K1	2.4 × 2.4	34.3	3	47	0.16
		K2	2.4 × 2.4	34.3	4	59	0.14
		K3	2.4 × 2.4	40.0	21	59	0.58
		K4	2.4 × 2.4	46.7	18	60	0.52
Zeynalian et al. [7]		K1	2.4 × 2.4	19.0	3	59	0.09
		K2	2.4 × 2.4	19.0	3	60	0.07
		K3	2.4 × 2.4	19.0	3	53	0.07
		K4	2.4 × 2.4	23.2	3	28	0.22
		K5	2.4 × 2.4	19.0	2	37	0.10
		K6	2.4 × 2.4	26.5	3	60	0.07
		K7	2.4 × 2.4	26.5	3.2	60	0.08
		K8	2.4 × 2.4	22.7	3	55	0.09
		K9	2.4 × 2.4	28.7	5	35	0.21
		K10	2.4 × 2.4	22.7	3	39	0.08
		K11	2.4 × 2.4	31.4	3.3	12	0.64
		K12	2.4 × 2.4	30.6	5	35	0.24
Sharafi et al., [28]	Hybrid	V	3.6 × 3.0	99.7	8	75	0.15
Sharafi et al., [29]		HWPS	3.6 × 3.0	115.4	20	75	0.39
This Study	Hybrid	HW-C2	2.4 × 2.4	54.3	43.5	60	1.46
		HW-C3	2.4 × 2.4	65.1	54.5	60	1.44

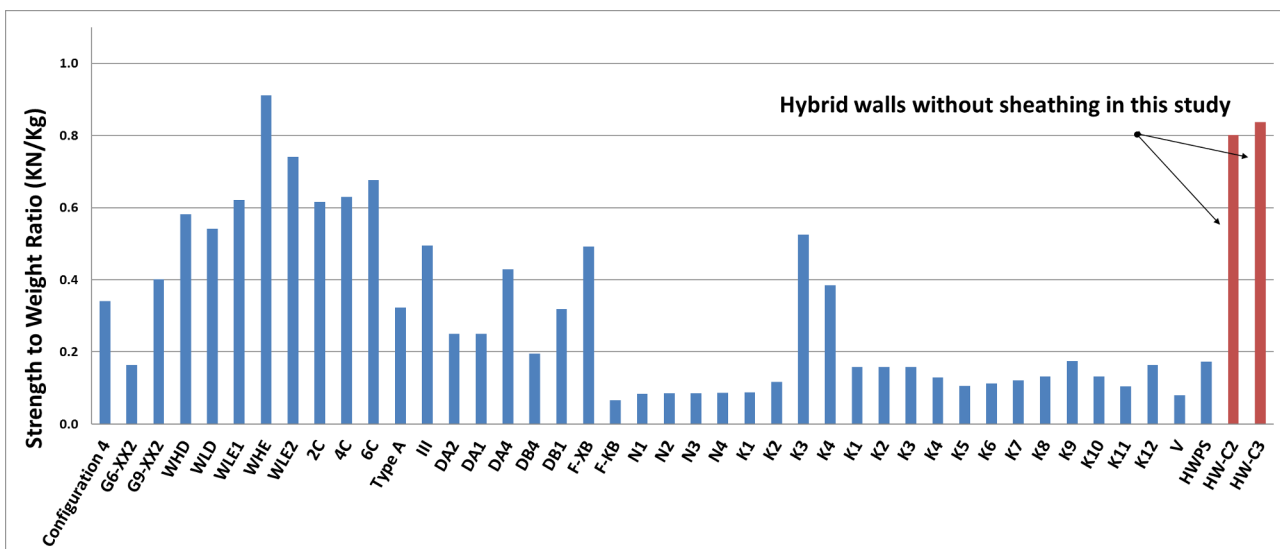


Fig. 11. Comparison of strength to weight ratio for braced walls.

Table 7

Tested sheathed walls by different researchers.

Author, Reference	Sheathing type	Specimen ID	Span (m × m)	Frame weight (Kg)	Other material weight (Kg)	Total weight (Kg)	Maximum strength (KN)	Maximum displacement (mm)	Elastic Stiffness (KN/mm)
Balh et al, [12,51]	Steel	Specimen 11	2.44 × 2.44	36.3	71	107.2	39	27	3.2
Tone et al,[12,52]		Specimen 16	2.44 × 2.44	34.7	53	87.7	24	31	3
Gao and xiao,[11]	Ply bamboo	D-C-3	2.44 × 2.44	36.3	38.7	75	33	56	1.1
Zeynalian and Ronagh, [50]	FCB ^a	H1	2.4 × 2.4	14.9	86.4	101.3	29	40	1.2
Moghimi and Ronagh, [5]	GWB ^b	AB1	2.4 × 2.4	15.8	32	47.8	6.5	44	0.6
Peck et al. [53]		CB1	2.4 × 2.4	16.7	32	48.7	9	60	0.9
		GWB.4-12	2.44 × 2.44	31.4	51	82.4	11.7	23	1.5
		GWB.4-6	2.44 × 2.44	31.4	51	82.4	12.4	20	1.5
		GWB.4-4	2.44 × 2.44	31.4	51	82.4	11.2	44	1.5
		GWB.6-12	2.44 × 2.44	31.4	51	82.4	7.3	20	1.3
Morgan et al., [54]		12	2.44 × 2.44	23.8	51	74.8	6.1	32	1.5
		14	2.44 × 2.44	23.8	51	74.8	4.2	58	2
		16	2.44 × 2.44	23.8	51	74.8	3.5	45	1.5
		18	2.44 × 2.44	25.8	51	76.8	10.6	27	2
		20	2.44 × 2.44	23.8	51	78.8	3.6	47	1
Serrette and Ogunfunmi, [10]	Type B	2.44 × 2.44	33.4	77	110.4	25.3	38	3	
Pan and Shan, [49]	Type C	2.44 × 2.44	37.9	77	114.9	28.9	38	2.5	
	OSB ^c	FFM-G09-FO	2.4 × 2.4	63	27.7	90.7	16.7	53	1.2
		FFM-G09-FT	2.4 × 2.4	63	54	117	28.8	50	1.7
		FFM-G12-FO	2.4 × 2.4	63	36	99	2.4	55	1.1
		FFM-O09-FO	2.4 × 2.4	63	35	98	44	59	1.7
		FFM-O12-FO	2.4 × 2.4	63	42	105	49	60	1.6
Dubina, [46]	OSB I	3.6 × 2.44	120	51	171.1	51	19	4.2	
Liu et al., [55]		12	2.44 × 2.74	63	44.1	107.1	41	50	2
		14	2.44 × 2.74	63	44.1	107.1	36	49	2.2
	OSB, GWB	15	2.44 × 2.74	63	44.1	107.1	31	42	1.6
		13	2.44 × 2.74	63	89.5	152.5	44	50	1.8
	GWB	16	2.44 × 2.74	63	45.4	108.4	8	37	0.9
Wang, and Ye, [14]	GWB,CON ^d	WA1	3.6 × 3	50.7	107.3	158	96	29	15
	GWB,BMB ^e -CON	WA2	3.6 × 3	50.7	236.3	314	96	25	10.9
		WA3	3.6 × 3	73.5	236.3	336.8	98	34	11
	GWB,BMB, CON,	WB1	3.6 × 3	134.7	498	632	76	43	19
	ALC ^f	WB2	3.6 × 3	97.1	498	595.1	123	47	23
YE et al., [56]	GWB, CSB ^g	Specimen 1	3.6 × 3	50.7	470	520.7	93	38	10.7
		Specimen 2	3.6 × 3	54.7	470	524.7	79	30	10.7
	GWB, BMB	Specimen 4	3.6 × 3	63.8	384	447.8	73	28	10.3
		Specimen 5	3.6 × 3	97.1	384	481.1	101	75	10.7
		Specimen 6	3.6 × 3	119.7	384	503.7	94	36	10.7
Xu et al., [15]	SB ^h	WA-1	2.4 × 3	43.5	288	331.5	37	33	4.1
	SB, LFC ⁱ	WB-1	2.4 × 3	43.5	623	666.5	88	60	10
		WB-2	2.4 × 3	43.5	748	791.5	106	44	11.8
		WB-3	2.4 × 3	65.3	622	687.3	96	57	15
		WC-1	2.4 × 3	62.1	810	872.1	107	50	13.5
		WC-2	2.4 × 3	62.1	810	872.1	110	48	14
This study	GWB	HW-C4	2.4 × 2.4	65.1	66.4	131.5	59	60	2.4

^a Fibre cement board.^b Gypsum wall board.^c Oriented strand board.^d Fine aggregate concrete (infilled material).^e Bolivian magnesium board.^f Autoclaved lightweight concrete slab.^g Calcium silicate board.^h Straw board.ⁱ Lightweight foamed concrete (infilled material).

and displacement of the frame. Hence, a lower R factor value might be obtained for a CFS wall with higher shear strength and lateral drift compared to another wall specimen. For example, the results reveal that while the maximum shear capacity of HW-C3 is higher than HW-C1 and HW-C2, the R factor of the latter walls is more than the former. This concern has also been reported by other researchers when they compared the R factor with the corresponding strength [4,7,48].

Accurately comparing the results of Table 8 and Table 5 indicates that the higher shear capacity of specimen HW-C3, compared to the HW-C1 and HW-C2, is not reflected by the test-based R factor values. Since the seismic design and base shear of a building directly depend on the R factor, the unreliable test-based R factor of a specimen like HW-C3 can lead to a building with overdesigned sections. In other words, the unique capability of a wall with high lateral capacity and ductility is

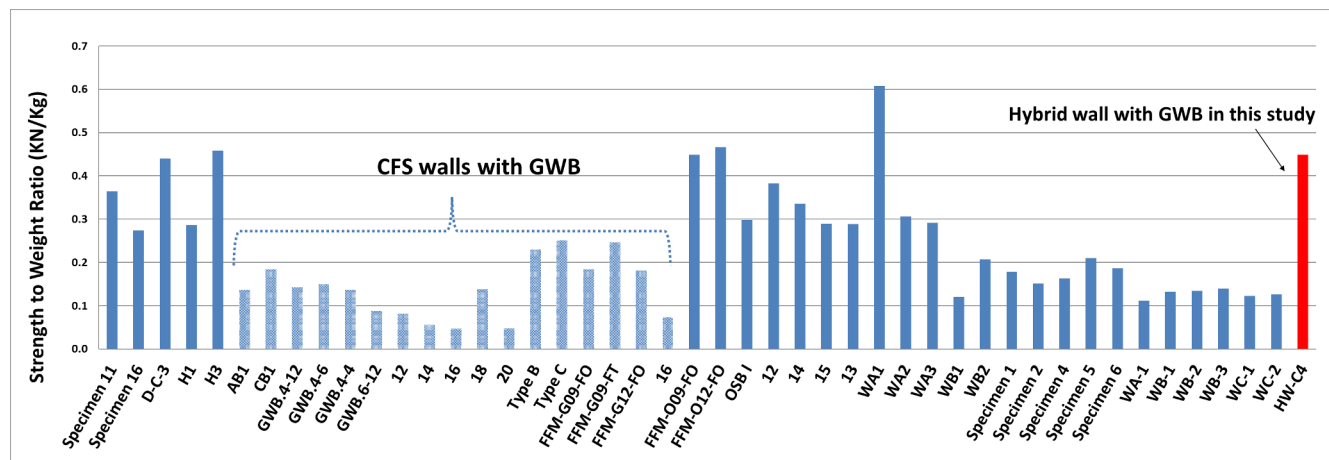


Fig. 12. Comparison of strength to weight ratio for sheathed walls.

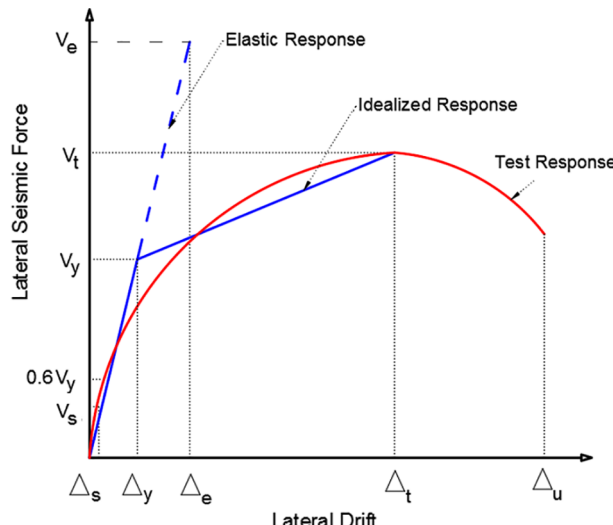


Fig. 13. Idealized bilinear curve for calculation of R factor.

not necessarily included in the test-based overstrength and ductility reduction factors, respectively. Since the test-based R factor of specimen HW-C3 limits the potential benefits of this system in design, the R factor values need to be determined using more sophisticated methods such as FEMA P-695 [57] methodology which determines the R factor through nonlinear response history analyses.

6. Conclusion and recommendations

This study provided the results of six full-scale hybrid CFS walls

under cyclic lateral loading and investigated the seismic characteristics of the system, such as response modification factor. Based on the cyclic test results, the following conclusions can be drawn:

- The test results indicated that the direction of SHS truss frame in the panel would not considerably affect the performance of the walls. In contrast, implementation of a single upright SHS at the other end of the panel led to reasonably better ductility and energy-absorbing capabilities than those without single SHS.
- Comparing seismic behaviour of hybrid specimen with sheathing (HW-C4) against the bare hybrid panel (HW-C3) also showed that strength and ductility of the wall were increased when GWB was used as a finishing material.
- It was also observed that shear strength and stiffness of specimens without truss brace configuration was not reasonable and therefore not recommended to be used for mid-rise structures.
- The R factor evaluation was performed through data analysing, and the average values of 6.1 and 7 were obtained for sheathed and unsheathed braced walls, respectively. Besides, specimen HW-C4 with GWB provided a higher R factor value than those CFS walls with sheathing material listed in the CFS regulations.
- Comparison of S/W ratio of CFS walls showed that the innovative solution of using SHS truss-braced design is deemed satisfactory for high seismic regions. It was also demonstrated that specimen HW-C3 as a braced wall and HW-C4 as a sheathed wall were adequately competent for a lateral-resistant system in modular mid-rise buildings, considering their lower weight compared to several massive walls.

The hybrid CFS construction industry is a new topic which is at its early stage of research. Further research should be performed over time

Table 8

Test-based R factor values determined based on FEMA.

Specimen	Overstrength factor (Ω_0)			Ductility factor (R_u)			Response modification factor (R)		
	Push	Pull	Average	Push	Pull	Average	Push	Pull	Average
HW-C1	3.1	4.5	3.8	2.3	1.5	1.9	7.2	6.9	7.1
HW-C2	4.4	2.6	3.5	1.5	1.9	1.7	6.9	5.1	6.0
HW-C3	3.2	3.8	3.5	1.6	1.5	1.6	5.1	5.7	5.4
HW-C4	5.3	4.1	4.7	1.4	1.6	1.5	7.5	6.5	7.0
HW-C5	1.2	1.6	1.4	3.8	3.4	3.6	4.6	5.3	4.9
HW-C6	1.4	1.5	1.5	3.3	3.5	3.4	4.8	5.4	5.1

through a continuous process to compile a comprehensive database for CFS buildings and to promote their application in actual mid-rise construction.

Declaration of Competing Interest

The authors declare that they have no known competing financial interests or personal relationships that could have appeared to influence the work reported in this paper.

Acknowledgements

This research is supported by an Australian Government Research Training Program (RTP) Scholarship.

References

- [1] Usefi N, Sharafi P, Ronagh H. Numerical models for lateral behaviour analysis of cold-formed steel framed walls: State of the art, evaluation and challenges. *Thin-Walled Struct* 2019;138:252–85.
- [2] Sharafi P, et al. Lateral force resisting systems in lightweight steel frames: Recent research advances. *Thin-Walled Struct* 2018;130:231–53.
- [3] Fiorino L, Terracciano MT, Landolfo R. Experimental investigation of seismic behaviour of low dissipative CFS strap-braced stud walls. *J Constr Steel Res* 2016;127:92–107.
- [4] Iuorio O, et al. Seismic response of Cfs strap-braced stud walls: Experimental investigation. *Thin-Walled Struct* 2014;85:466–80.
- [5] Moghimi H, Ronagh HR. Performance of light-gauge cold-formed steel strap-braced stud walls subjected to cyclic loading. *Eng Struct* 2009;31(1):69–83.
- [6] Pourabdollah O, Farahbod F, Rofooei FR. The seismic performance of K-braced cold-formed steel shear panels with improved connections. *J Constr Steel Res* 2017;135:56–68.
- [7] Zeynalian M, Ronagh HR, Hatami S. Seismic characteristics of K-braced cold-formed steel shear walls. *J Constr Steel Res* 2012;77:23–31.
- [8] Shafeai S, Ronagh H, Usefi N. Experimental evaluation of CFS braced-truss shear wall under cyclic loading. *Advances in Engineering Materials, Structures and Systems: Innovations, Mechanics and Applications: Proceedings of the 7th International Conference on Structural Engineering, Mechanics and Computation (SEMC 2019)*, September 2-4, 2019, Cape Town, South Africa. CRC Press; 2019.
- [9] Accorti M, et al. Reprint of response of CFS sheathed shear walls. *Structures* 2016;8:318–30.
- [10] Serrette R, Ogunfunmi K. Shear resistance of gypsum-sheathed light-gauge steel stud walls. *J Struct Eng* 1996;122(4):383–9.
- [11] Gao WC, Xiao Y. Seismic behavior of cold-formed steel frame shear walls sheathed with ply-bamboo panels. *J Constr Steel Res* 2017;132:217–29.
- [12] DaBreo J, et al. Steel sheathed cold-formed steel framed shear walls subjected to lateral and gravity loading. *Thin-Walled Struct* 2014;74:232–45.
- [13] Tian H-W, Li Y-Q, Yu C. Testing of steel sheathed cold-formed steel trussed shear walls. *Thin-Walled Struct* 2015;94:280–92.
- [14] Wang X, Ye J. Reversed cyclic performance of cold-formed steel shear walls with reinforced end studs. *J Constr Steel Res* 2015;113:28–42.
- [15] Xu Z, et al. Seismic performance of high-strength lightweight foamed concrete-filled cold-formed steel shear walls. *J Constr Steel Res* 2018;143:148–61.
- [16] Liu B, et al. Performance of cold-formed-steel-framed shear walls sprayed with lightweight mortar under reversed cyclic loading. *Thin-Walled Struct* 2016;98:312–31.
- [17] Schafer B, et al. Seismic response and engineering of cold-formed steel framed buildings. *Structures* 2016;8:197–212.
- [18] Fiorino L, Macillo V, Landolfo R. Shake table tests of a full-scale two-story sheathing-braced cold-formed steel building. *Eng Struct* 2017;151:633–47.
- [19] Kim T-W, et al. Shaketable tests of a cold-formed steel shear panel. *Eng Struct* 2006;28(10):1462–70.
- [20] Fiorino L, Bucciero B, Landolfo R. Shake table tests of three storey cold-formed steel structures with strap-braced walls. *Bull Earthq Eng* 2019;17(7):4217–45.
- [21] Leng J, et al. Modeling seismic response of a full-scale cold-formed steel-framed building. *Eng Struct* 2017;153:146–65.
- [22] Franklin NP, et al. Efficient 3D lateral analysis of cold-formed steel buildings. *J Constr Steel Res* 2019;160:16–22.
- [23] Campiche A, et al. Seismic behaviour of strap-braced LWS structures: shake table testing and numerical modelling. *IOP Conference Series: Materials Science and Engineering*. IOP Publishing; 2019.
- [24] Fiorino L, et al. Seismic response of CFS shear walls sheathed with nailed gypsum panels: Numerical modelling. *Thin-Walled Struct* 2018;122:359–70.
- [25] Usefi N, et al. Macro/micro analysis of cold-formed steel members using ABAQUS and OPENSEES. *Volume of Abstracts, Proceedings of the 13th International Conference on Steel, Space and Composite Structures (SS18)*. 2018.
- [26] Usefi N, Ronagh HR, Mohammadi M. Finite element analysis of hybrid cold-formed steel shear wall panels. *Streamlining Information Transfer between Construction and Structural Engineering: Proceedings of the Fourth Australasia and South-East Asia Structural Engineering and Construction Conference, Brisbane, Australia, December 3-5, 2018*. 2018.
- [27] AISI, North American standard for seismic design of cold-formed steel structural systems; 2015.
- [28] Mortazavi M, et al. Lateral behaviour of hybrid cold-formed and hot-rolled steel wall systems: Experimental investigation. *J Constr Steel Res* 2018;147:422–32.
- [29] Mortazavi M, et al. Prefabricated hybrid steel wall panels for mid-rise construction in seismic regions. *J Build Eng* 2020;27:100942.
- [30] Usefi N, Ronagh H, Sharifi P. Lateral performance of a new hybrid CFS shear wall panel for mid-rise construction. *J Constr Steel Res* 2020;168:106000.
- [31] FEMA 365, Prestandard and Commentary for the Seismic Rehabilitation of Buildings in Rehabilitation Requirements. 2000, Federal Emergency Management Agency, Washington, D.C.
- [32] FEMA P-1050, NEHRP Recommended Seismic Provisions for New Buildings and Other Structures Volume I: Part 1 Provisions, Part 2 Commentary 2015, Building Seismic Safety Council, Washington, DC, 515 pp.
- [33] Uniform building code. 1997, International Conference of Building Officials, Whittier.
- [34] International building code. 2018: International Code Council.
- [35] ASCE/SEI 7, Minimum design loads and associated criteria for buildings and other structures, 2017. American Society of Civil Engineers Reston, VA.
- [36] National Building Code of Canada. 2015, National Research Council of Canada.
- [37] Eurocode 8: Design of structures for earthquake resistance. 2005, European Committee for Standardization.
- [38] AS/NZS 4600, Cold-formed steel structures. 2018, Standards Australia.
- [39] iccons, Screw Technical Guide. 2017: Australia.
- [40] ASTM E2126, Standard test methods for cyclic (reversed) load test for shear resistance of vertical elements of the lateral force resisting systems for buildings. 2019, ASTM International West Conshohocken, PA.
- [41] Sharifi M, et al. Estimation of moment and rotation of steel rack connections using extreme learning machine. *Steel Compos Struct* 2019;31(5):427–35.
- [42] Sharifi M, et al. A novel approach to predict shear strength of tilted angle connectors using artificial intelligence techniques. *Eng Computers* 2020;1:21.
- [43] Mohammadi M, et al. Experimental and numerical investigation of an innovative buckling-restrained fuse under cyclic loading. *Structures* 2019;22:186–99.
- [44] Ayatollahi SR, et al. Performance of gypsum sheathed CFS panels under combined lateral and gravity loading. *J Constr Steel Res* 2020;170:106125.
- [45] Sharifi P, et al. Identification of factors and decision analysis of the level of modularization in building construction. *J Arch Eng* 2018;24(2):04018010.
- [46] Dubina D. Behavior and performance of cold-formed steel-framed houses under seismic action. *J Constr Steel Res* 2008;64(7):896–913.
- [47] Al-Kharat M, Rogers CA. Inelastic performance of cold-formed steel strap braced walls. *J Constr Steel Res* 2007;63(4):460–74.
- [48] Zeynalian M, Ronagh HR. An experimental investigation on the lateral behavior of knee-braced cold-formed steel shear walls. *Thin-Walled Struct* 2012;51:64–75.
- [49] Pan C-L, Shan M-Y. Monotonic shear tests of cold-formed steel wall frames with sheathing. *Thin-Walled Struct* 2011;49(2):363–70.
- [50] Zeynalian M, Ronagh HR. Seismic performance of cold formed steel walls sheathed by fibre-cement board panels. *J Constr Steel Res* 2015;107:1–11.
- [51] Bahl N. Development of seismic design provisions for steel sheathed shear walls. *Masters Abstracts International*. 2010.
- [52] Ong-Tone, C., Tests and Evaluation of Cold-formed Steel Frame. 2009: Department of Civil Engineering and Applied Mechanics, McGill University.
- [53] Peck Q, Rogers N, Serrette R. Cold-formed steel framed gypsum shear walls: in-plane response. *J Struct Eng* 2012;138(7):932–41.
- [54] Serrette R, Morgan K, Sorhouet M. Performance of cold-formed steel-framed shear walls: Alternative configurations. Final Report: LGSRG-06-02, Santa Clara University, Santa Clara, CA; 2002.
- [55] Liu P, Peterman K, Schafer B. Test report on cold-formed steel shear walls; 2012.
- [56] Ye J, et al. Cyclic performance of cold-formed steel shear walls sheathed with double-layer wallboards on both sides. *Thin-Walled Struct* 2015;92:146–59.
- [57] FEMA P695, Quantification of Building Seismic Performance Factors 2009, Federal Emergency Management Agency, Washington, D.C.